Physics of the Earth and Planetary Interiors, 68 (1991) 85–96
Elsevier Science Publishers B.V., Amsterdam

Preliminary spectral analysis of the residual signal of a superconducting gravimeter for periods shorter than one day

N. Florsch [a], J. Hinderer [b], D.J. Crossley [b,1], H. Legros [b] and B. Valette [c]

[a] *Laboratoire de Géophysique Appliquée, Université P. et M. Curie, 4, place Jussieu, 75252 Paris Cedex 05, France*
[b] *Laboratoire de Géodynamique, IPG Strasbourg, 5 rue René Descartes, 67084 Strasbourg Cedex, France*
[c] *Laboratoire de Sismologie, IPG Paris, 4, place Jussieu, 75252 Paris Cedex 05, France*

(Received 28 June 1990; revision accepted 12 December 1990)

ABSTRACT

Florsch, N., Hinderer, J., Crossley, D.J., Legros, H. and Valette, B., 1991. Preliminary spectral analysis of the residual signal of a superconducting gravimeter for periods shorter than one day. Phys. Earth Planet. Inter., 68: 85–96.

We show for the first time an analysis of a 1.5 year data set from the superconducting gravimeter in Strasbourg. For periods between 7 and 24 h, a residual gravity signal is first generated by removal of the main tidal components by a standard least squares fit; this signal is then treated to suppress any remaining transient signals (de-spiking). At shorter periods, between 7 h and 10 min, a simple high-pass filter is applied before de-spiking. In both cases, the noise level is estimated in different frequency bands; spectra of the gravity residuals are shown. We also analysed by two different methods the local barometric pressure, which contains harmonic components of the S_1 wave related to air pressure changes — driven by diurnal solar heating — superimposed on the frequency-dependent meteorological noise. After removal of the daily harmonics which are also present in the gravity residual spectrum, a few remaining spectral lines of possible geophysical interest are discussed.

1. Introduction

A superconducting gravimeter (model GWR TT70) has been operating since February 1987, in a fort near Strasbourg built in 1875, called J9 (48.622° N, 7.684° E). After an initial period of instrumental tests, the gravity signal has been recorded digitally since July 1987 at a sampling interval of 5 min, with the barometric pressure, the water table level (in the well located below the station), two orthogonal tilt measurements and the internal temperature of the gravity sensing unit in the helium bath also being recorded. The gravity signal is digitized every 2 s and convolved with a low-pass, anti-aliasing filter of 20 min length. The data used in this study are taken from a 1.5 year acquisition period from 1 January 1988 to 31 May 1989.

The aim of this preliminary study is to investigate the lower limit of the gravity noise of a superconducting gravimeter record, inside and outside the tidal bands, which can be obtained after removing the known signals; these are essentially the lunisolar tidal variations (typically of the order of 100 μgal in the present case), in addition to the gravity change induced by the fluctuating barometric pressure (typically about 15 μgal for a 45 mbar change). Therefore, in order to benefit from the very high sensitivity of the cryogenic gravimeter (of the order of a nanogal) for detecting a new gravimetric phenomenon, it is especially important to carefully remove the tidal components from the signal. It will be shown that with a noise level of several nanogal (for periods below one day), the superconducting gravimeter is an

[1] Permanent address: Department of Geological Sciences, McGill University, Montreal, Canada.

0031-9201/91/$03.50

extremely useful tool for studying important geodynamic problems like the long-period (subseismic) core modes of gravity-inertial origin (Melchior and Ducarme, 1986; Zürn et al., 1987; Melchior et al., 1988; Mansinha et al., 1990) or the translation of the solid inner core (Slichter mode). Of course, any (non-tidal) oscillation in the atmosphere (or even the oceans) in the same frequency range (see, for example, Volland, 1988) can also lead to gravity changes which can be observed with this type of instrument (see also Hinderer and Legros 1989).

At periods between 7 and 24 h, tides are first subtracted after a least-squares estimate of their amplitudes and phases. At shorter periods, a simple high-pass filter is applied. In both cases, a residual signal is generated which is then analysed in the frequency domain. At this first stage, the residuals contain transient signals (spikes and glitches), which are due to different kinds of perturbations (instrumental, earthquakes or gaps in the record). The energy corresponding to these undesirable impulses is spread over the whole frequency range. It leads to errors in the precise determination of the amplitudes and phases of the tidal waves that were eliminated and can consequently mask small spectral lines. In a second stage, these spikes are removed by a de-spiking procedure: the signal is forced to zero every time it exceeds a given threshold. This threshold is chosen by a close inspection of the histogram of the residuals. Afterwards, a final spectral analysis is undertaken, which suggests the presence of some spectral peaks of geophysical interest.

2. Analysis for periods between 7 and 24 h

For analysing the gravity signal in the period range between 7 and 24 h, the signal is first re-sampled at hourly intervals in order to use a standard least squares tidal analysis code. The re-sampling is performed with an efficient Finite Impulse Response (FIR) filter to prevent aliasing.

In a least-squares tidal fit, the observed tidal signal is usually compared with the theoretical one computed for a rigid body by introducing the well-known gravimetric factors δ and phase shifts κ (Melchior, 1983). In principle, this analysis is applied to any possible tidal wave but, because of the finite length of the record and hence the limited frequency resolution, the theoretical tide is expressed as the sum over a finite number n of wave groups (Schüller, 1977):

$$s_0(t) = \sum_{i=1}^{n} \delta_i \cos \kappa_i \sum_{j=1}^{m_i} A_{ij} \cos(\omega_{ij} t + \phi_{ij}) - \sum_{i=1}^{n} \delta_i \sin \kappa_i \sum_{j=1}^{m_i} A_{ij} \sin(\omega_{ij} t + \phi_{ij}) \quad (1)$$

In this expression, A_{ij} and ϕ_{ij} are respectively the theoretical amplitude and phase of the wave j in group i (m_i is the number of individual waves in a given group i) with angular frequency ω_{ij}.

In fact, the observed gravity signal $s(t)$ can be decomposed into the following sum:

$$s(t) = s_0(t) + n(t) + e(t) + d(t) + b(t) \quad (2)$$

where $s_0(t)$ is the theoretical tide (1), $n(t)$ is a coloured noise (e.g. microseismic noise) and $e(t)$ represents disturbances (e.g. earthquakes, instrumental perturbations). Since these perturbations only occur at short time intervals (say less than a few hours), they appear as spikes with respect to the 1.5 year gravity signal; hereafter we reserve the term 'spike' for this kind of short transient signal. $d(t)$ is the drift of the instrument, usually modelled by a polynomial of degree 1–3 (Richter, 1983). $b(t)$ contains physical gravity signals which, in principle, can be modelled like the ones caused by atmospheric pressure, water table level fluctuations and tilts of the building, etc.

The least-squares tidal analysis attempts to minimize the integral (T being the duration of observation):

$$F(\{\delta_i\}, \{\kappa_i\}) = \int_T [s(t) - s_0(t) - d(t) - b(t)]^2 \, dt$$

with respect to the tidal parameters δ_i, κ_i contained in $s_0(t)$. Other parameters contained in $b(t)$ can either be assumed a priori or added as unknowns in the global analysis; an example is the barometric admittance which can be found simultaneously when adjusting the tides (e.g.

Schüller 1986). The noise $n(t)$ represents all stochastic processes which cannot be modelled physically. Its energy is spread over the time domain as well as the frequency domain; because of this spreading, it cannot be reduced without affecting the amplitudes and phases of the tides. Consequently it will limit the accuracy that can be attained in any tidal analysis. For a given spectral line at a particular frequency, this accuracy depends directly on the level of noise around the line. On the other hand, the noise $e(t)$ also has energy over the whole frequency range, but is concentrated in short time intervals. Therefore, it can be reduced by applying a de-spiking process in these intervals.

The following procedure has been developed to remove the 'spike' signal $e(t)$ from the observed gravity in order to obtain a gain in accuracy when determining the amplitudes and phases of the tides. The hourly data are first high-pass filtered (using a cut-off period of 4 days) to remove any low-frequency components (drift, long-period tides, polar motion). A standard tidal analysis (HYCON, Schüller, 1977) is done to provide a first estimate of the δ and κ parameters. A three-term convolution filter is used to correct for the effect of the local barometric pressure on gravity. The histogram of the time-dependent gravity residuals (which are the differences between the observed and modelled signals) is computed. The tails of this distribution represent large amplitude spikes which cannot be considered to contain useful information. A threshold is chosen, in our case 1 μgal, beyond which we force the signal to be zero; the difference between the time-dependent raw data and the despiked data is called the DSF (de-spiking function). The reduction in the noise level of the amplitude spectrum due to this de-spiking procedure, especially outside the tidal bands, is significant (see Fig. 1a and Appendix). In the diurnal and semi-diurnal bands, the tides have not been completely removed. This stems from the loss of accuracy in the estimate of the tidal amplitudes and phases, as mentioned above.

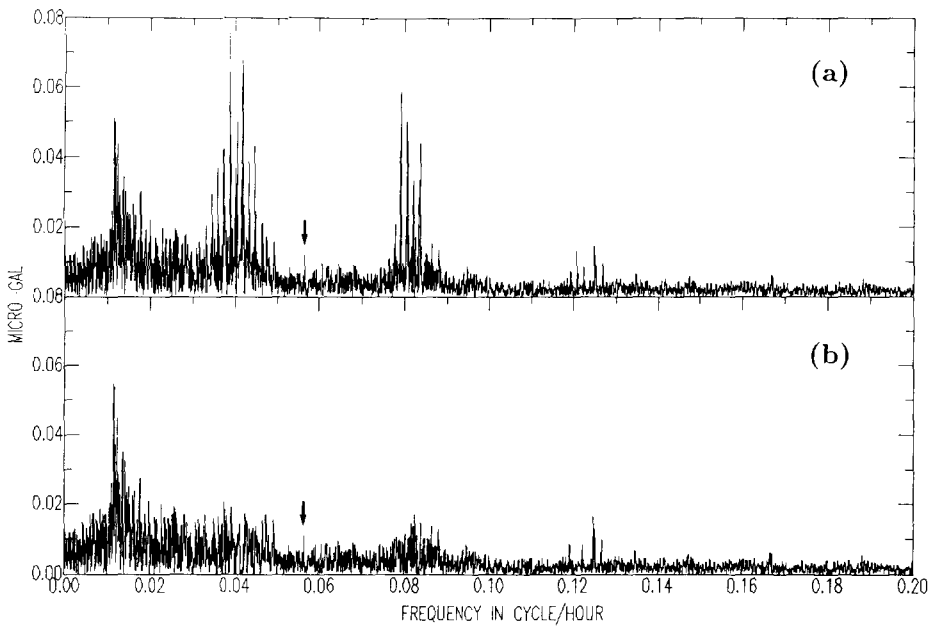

Fig. 1. Amplitude spectra of the gravity residuals. (a) After de-spiking. (b) After a second tidal analysis using the corrected gravity signal (original data minus de-spiking function). The low frequency noise (below 0.01 cycles h^{-1}) generated by the de-spiking procedure is not significant. The tides are clearly attenuated after the second analysis. The only (non-tidal) spectral line, slightly above the ambient noise, at 17.7 h (amplitude 12 nanogal), is indicated.

In a second processing stage the DSF is subtracted from the original gravimetric data, so that this signal no longer contains large spikes, and a second tidal analysis is performed. Figure 1b shows the spectrum (after applying a Hann window and $8 \times$ zero padding) of the new residuals after the second analysis. The residual tidal signals (diurnal band about 0.04 cycle h^{-1}, semi-diurnal band about 0.08 cycle h^{-1} and ter-diurnal band about 0.12 cycle h^{-1}) are clearly reduced. The noise level reaches about 20 nanogal in the tidal band and a few nanogal outside. The energy below 0.0105 cycles h^{-1} is not significant: it consists only of the low-frequency noise generated on the filtered gravity signal by the de-spiking procedure itself. In Fig. 1, there is only one possible non-tidal spectral line at 0.0565 cycles h^{-1} (17.7 hour period), which appears slightly above the ambient residual noise, with an amplitude of about 12 nanogal. Notice that a spectral line with similar features can be found in the residual gravity signal recorded by two Lacoste–Romberg spring gravimeters in Schiltach (Germany) equipped with electrostatic feedback (Wenzel and Zürn, 1990). The 13.89 hour peak, which was initially detected in the Brussels spectrum by Melchior and Ducarme (1986), but was not present in the record from the superconducting gravimeter in Bad Homburg 300 km away (Zürn et al., 1987), does not appear in our data. The spectral range of Fig. 1 has also been investigated recently by Mansinha et al. (1990) using a 4 year record from the Brussels superconducting gravimeter. These authors did not find any statistically significant non-tidal peak in the band between 12 and 24 h.

3. Comments on the atmospheric pressure

We analysed the 1.5 year local barometric pressure changes using the raw 5 min sampling interval. It is well known that the pressure spectral content is highly frequency dependent, the mean amplitude decreasing with increasing frequency. The amplitude spectrum of the twice-differentiated pressure signal with respect to time (this is equivalent to applying a high-pass filter having a transfer function proportional to f^2, where f is the frequency) is given in Fig. 2 on a linear scale. We have indicated the spectral lines which clearly

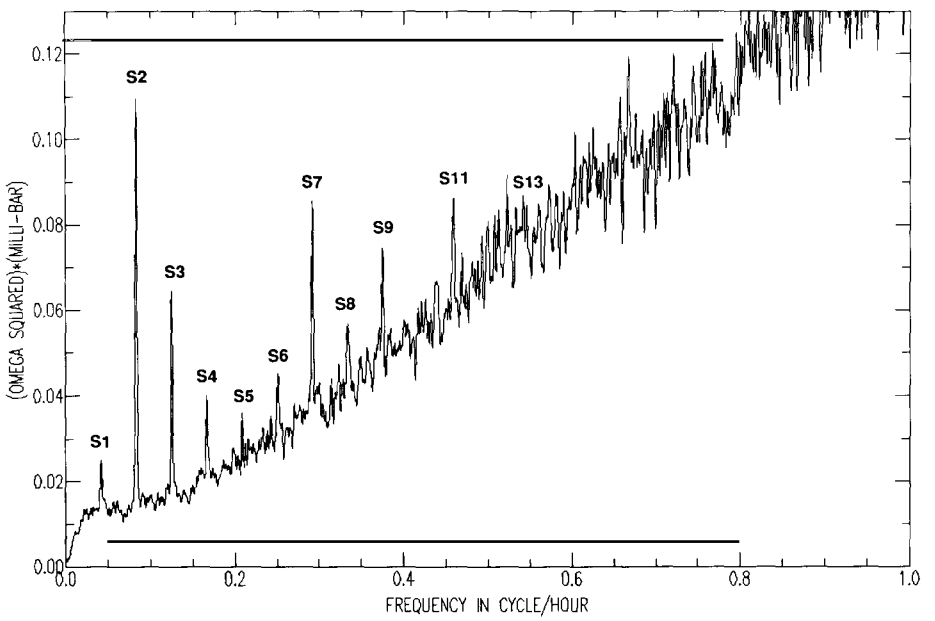

Fig. 2. Amplitude spectrum of the second time derivative of the pressure. Harmonics of the solar day S_1 are visible up to S_{13}.

superimpose on the meteorological noise: these are the harmonic components of the solar day S_1 like S_2, S_3... up to S_{13}, which are a well-known feature of pressure spectra (Warburton and Goodkind, 1977; Spratt, 1982). The almost linear slope in the background noise for frequencies higher than 3 cycles day^{-1} confirms that the pressure spectrum itself varies as $1/f$ in this frequency range, being comparable to the statistical behaviour of a 1-D Brownian noise. However, the noise seems to be more or less constant for frequencies below 3 cycles day^{-1}, suggesting rather a $1/f^2$ dependence. Notice also that the mean amplitude of the daily harmonic lines seems to be only weakly dependent on frequency. Therefore, they are clearly visible up to S_{13}, but would be hidden at higher frequencies (if they exist) by the meteorological noise. The top curve of Fig. 3 shows the amplitude spectrum of the pressure on a logarithmic scale, between 0.01 cycles h^{-1} and 6 cycles h^{-1} (our Nyquist frequency). The change in the slope of the background noise from a value close to -2 for frequencies below 3 cycles day^{-1} to a value of -1 for higher frequencies (except perhaps for frequencies larger than 3 cycles h^{-1}), as mentioned above in Fig. 2, is confirmed. The bottom of Fig. 3 shows the amplitude spectrum of the pressure signal which is stacked in the time domain (see Fig. 4). Since the meteorological noise is not coherent from one day to the other, we performed this simple experiment to provide an insight into the frequency decrease of the harmonics of S_1. Because we are dealing with exact multiples of one cycle per solar day, we stacked the pressure time signal by taking intervals of exactly one day. With 600 days available, the noise is reduced by a factor of $(600)^{1/2} \approx 25$. Then a new signal is created by repeating 600 times the same daily signal and Fourier transforming it (this enables us to perform the procedure exactly over the same duration as for the raw pressure signal). The spectral lines of Fig. 3 evidently correspond to the

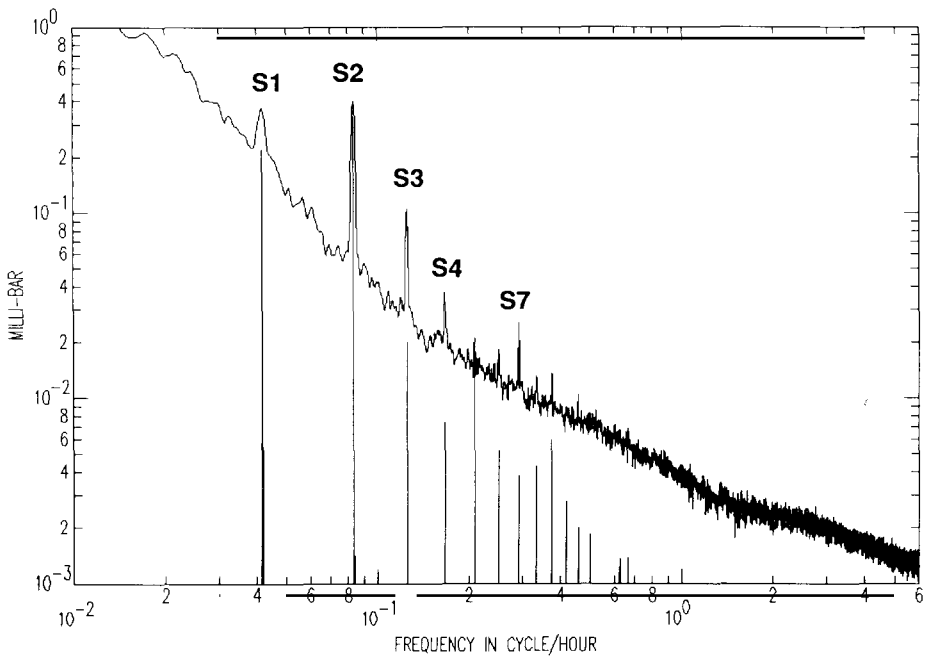

Fig. 3. Amplitude spectra of the pressure. The top curve represents the spectrum of the raw pressure signal (obtained by averaging 39 windows of 30 days, each with a 50% overlap). The lower part shows the spectral content of the pressure signal stacked over 600 intervals of one day. The lowest harmonics of S_1 are readily apparent.

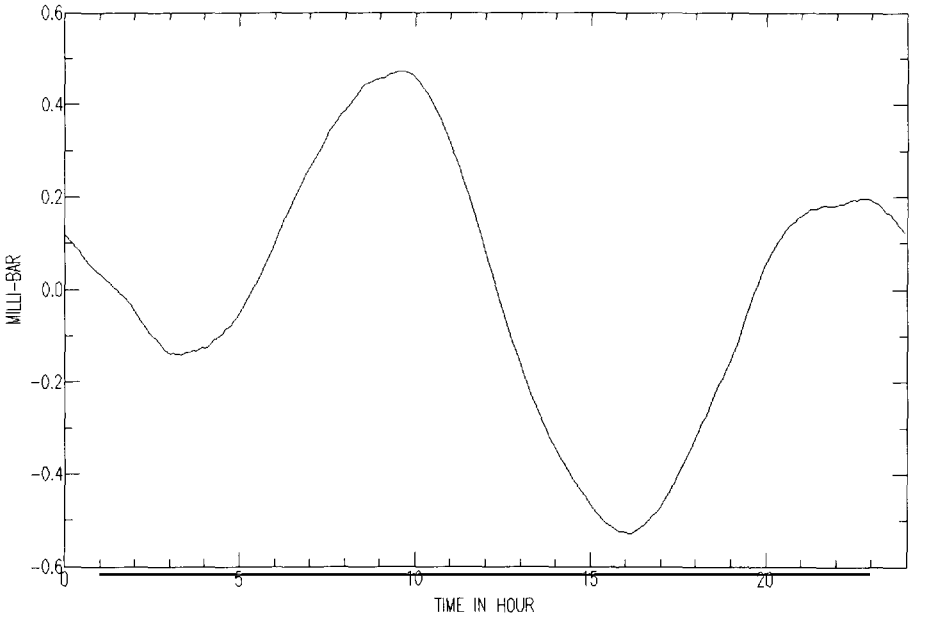

Fig. 4. Mean value of the daily pressure obtained by stacking 600 successive intervals of exactly one day.

harmonics of the solar day, which seem to be present up to 0.54 cycles h^{-1} (S_{13}).

4. Analysis for periods below 7 h

In the analysis for periods shorter than 7 h we start from raw gravity and pressure data sampled every 5 min. The gravity signal is first corrected for the local barometric pressure with a constant (frequency-independent) admittance factor (0.3 μgal $mbar^{-1}$). We take the first derivative of the gravity signal with respect to time and apply a high-pass filter (using a cut-off period of 7 h) in order to remove the tidal constituents. From the histogram of the filtered signal, a threshold of 0.07 gal is chosen and the de-spiking procedure is undertaken. Finally, a spectral analysis is performed by using the periodogram method (ten windows of three months with 50% overlap). Since the natural decrease of the gravity spectrum is proportional to $1/f$, it is useful to take the derivative of the signal to compensate for this decrease (a classical procedure called pre-whitening). The frequency dependence of the gravity noise spectrum is of course directly related to that of the local barometric pressure. It should be stated that the spectra of the undifferentiated, high-pass-filtered signal and its first time derivative show similar features, supporting the existence of some spectral lines that will be discussed later.

For periods less than 7 h, the de-spiking procedure reduces the gravity noise by a factor close to 4 (i.e. 12 dB). The existence of spectral lines which were previously hidden in the noise due to the spikes, is shown in the gravity spectrum (after differentiation) plotted in the upper part of Fig. 5. The noise below 0.143 cycles h^{-1} (using a cut-off period of 7 h) introduced by the de-spiking procedure is not significant. Most of the spectral lines are harmonics of the solar day and this appears clearly in the lower part of Fig. 5, from which they have been removed. The average noise level in gravity around a given frequency f can be easily obtained by dividing the amplitude of Fig. 5 by $\omega = 2\pi f$. Evidently, some of the low frequency gravity harmonics are connected with the same harmonics in the pressure (see Fig. 2). Because of

the large spatial extent of the pressure distribution of the harmonics of S_1 (Haurwitz and Cowley, 1973; Kikuchi, 1971; Legros and Hinderer, 1990; Van Dam and Wahr, 1987), the induced gravity changes may be different from those caused by local meteorological fluctuations (Warburton and Goodkind, 1977; Hinderer and Legros, 1989) which are corrected here with the help of a constant barometric admittance. The related problem of the admittance of gravity to pressure for atmospheric tides (from S_1 to S_{13}) will be investigated in more detail elsewhere. However, local effects (such as harmonics of the diurnal water table level fluctuations or tilt of the building due to solar heating), can also be the source of some (if not all) of these harmonic constituents (especially towards the higher frequencies). We see that there is an accumulation of peaks at certain preferred frequencies, especially 1 cycles h^{-1} and 2 cycles h^{-1}; the lines on either side of these frequencies can be produced by long-period (e.g. diurnal) modulation of an hourly effect. There is an individual spectral line at 4 cycles h^{-1} (S_{96} of 15 min period), which we also found in tilt measurements; we therefore suspect this peak to be of artificial origin (e.g. periodicity in the thermal regulation of the gravimeter room).

We can comment briefly on a possible interaction between some of the high frequency ($\geqslant 1$ cycles h^{-1}) harmonic constituents of the barometric pressure and seismic normal modes; for instance, the mode ${}_3S_2$ has an eigenperiod of 15.05 min (for the model 1066A), which is very close to the solar harmonic S_{96}. Suppose, in addition, that S_{96} has a $P_2^m(\cos\theta)\cos m\lambda$ surface amplitude distribution as ${}_3S_2$ does, where θ is the co-latitude, λ the longitude and $P_n^m(\cos\theta)$ the associated Legendre polynomial of degree n and order m. Then, one could imagine, in principle, that the 15 min pressure-induced gravity signal might be strongly amplified by a resonance process with ${}_3S_2$ to a level observable in the residual gravity spectrum. But, in fact, this hypothesis probably does not hold because it is likely to be impossible to find high frequency changes in the atmospheric pressure which are coherent over large spatial

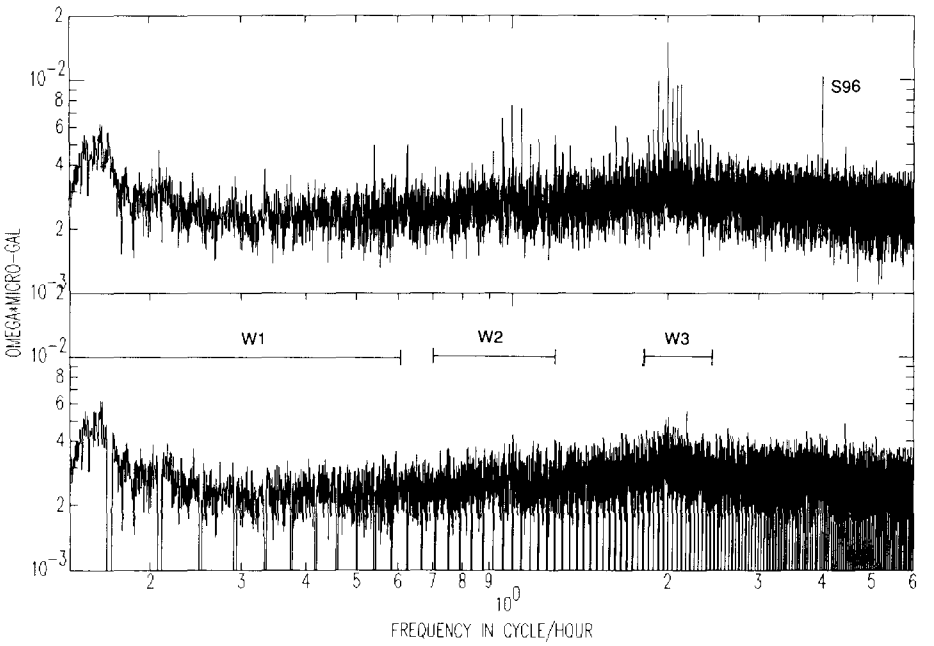

Fig. 5. Spectrum of the first time derivative of the gravity after high-pass filtering and de-spiking. In the lower part, daily harmonics have been removed. The low-frequency noise (below 0.14 cycles h^{-1}) generated by the de-spiking procedure is not significant.

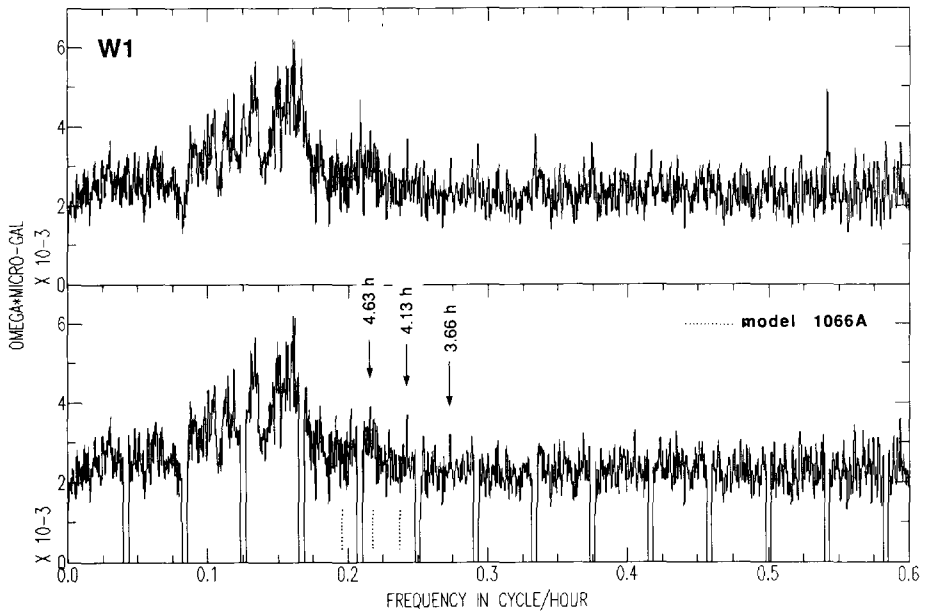

Fig. 6. Magnification of window W1 from Fig. 5. In the lower part, daily harmonics have been removed. The arrows indicate a triplet slightly above the ambient noise. The dotted lines are the theoretical frequencies of the Slichter mode of the inner core (for model 1066A).

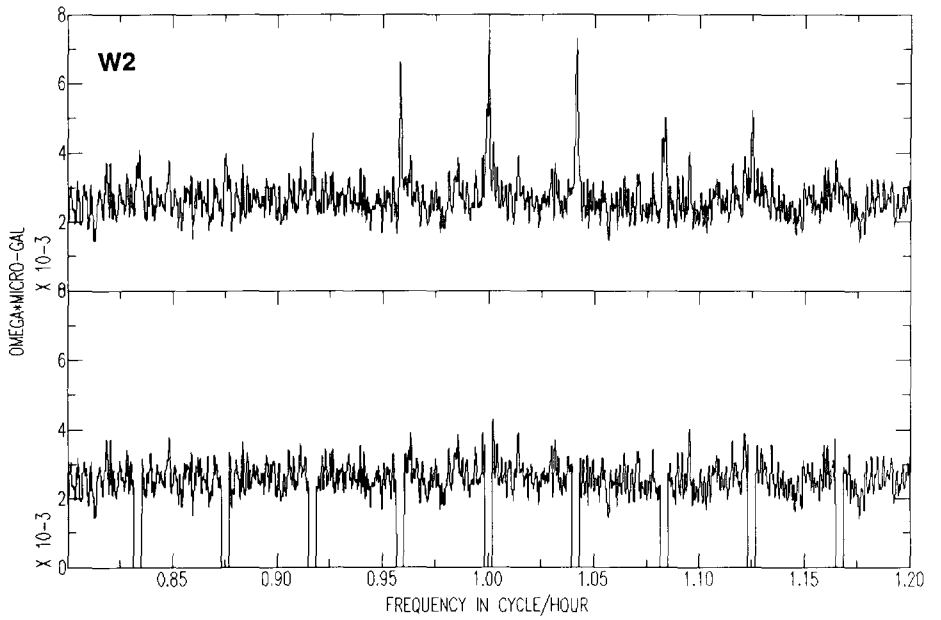

Fig. 7. Magnification of window W2 from Fig. 5. In the lower part, daily harmonics have been removed.

wavelengths. As shown by Chapman and Lindzen (1970) for the spherical harmonic expression of the lowest harmonics of the global pressure field (S_1 – S_4), we must always have the relationship $n \geqslant m$ for the surface distribution P_n^m (cos θ) cos $m\lambda$ relative to a harmonic wave S_m of frequency $2\pi m/T$, where T is one solar day. Extrapolating this fact towards the higher harmonics means that, in the case of S_{96}, we would have an azimuthal number $m = 96$ and a degree $n \geqslant 96$ (wavelength $\leqslant$ 400 km) and no interaction at all with the degree $n = 2$ seismic normal mode of almost identical frequency. In another context, one could also imagine an atmospheric cause (sudden change in air pressure or load during a synoptic storm, for instance) of excitation of seismic normal modes. This could be another explanation (quite unlikely for energy reasons) for anomalous excitation of free oscillations of the Earth which are not associated with significant seismic events and attributed to 'silent earthquakes' (Beroza and Jordan, 1990). However, the coupling between the Earth and its atmosphere has to be studied in more detail, especially with respect to the boundary conditions to be applied for this type of excitation.

The three windows W1, W2 and W3 indicated in Fig. 5 are magnified in Figs. 6, 7 and 8, respectively. The first window W1 ranges from 0 to 0.6 cycles h^{-1} (in fact, the lower frequency limit is 0.143 cycles h^{-1} because of the cut-off period of the high-pass filter). The lower part of Fig. 6 is identical to the top part, but the harmonics of the solar day have been eliminated to emphasize the existence of other possible spectral lines. A triplet indicated by arrows seems to emerge from the ambient noise with periods of 4.63, 4.13 and 3.66 h. We first checked that this triplet was not present in the pressure spectrum. Notice that the triplet appears on a spectrum stacked over ten windows of 3 months with 50% overlap. No clear correlation in time with earthquakes of magnitude greater than 7 which occurred during data acquisition was found. For comparison, we have indicated by dotted lines the frequencies of the three theoretical Slichter modes (translation mode of the inner core, split by rotation), calculated by Dahlen and Sailor (1979) for the Earth model 1066A. The actual amplitudes of the triplet can be obtained by dividing the amplitudes on Fig. 6 by ω. For instance, the central peak at 4.13 hour (248 min) has a real amplitude of $3.8 \times 10^{-3}(0.242.\ 2\pi)^{-1} = 2.5$

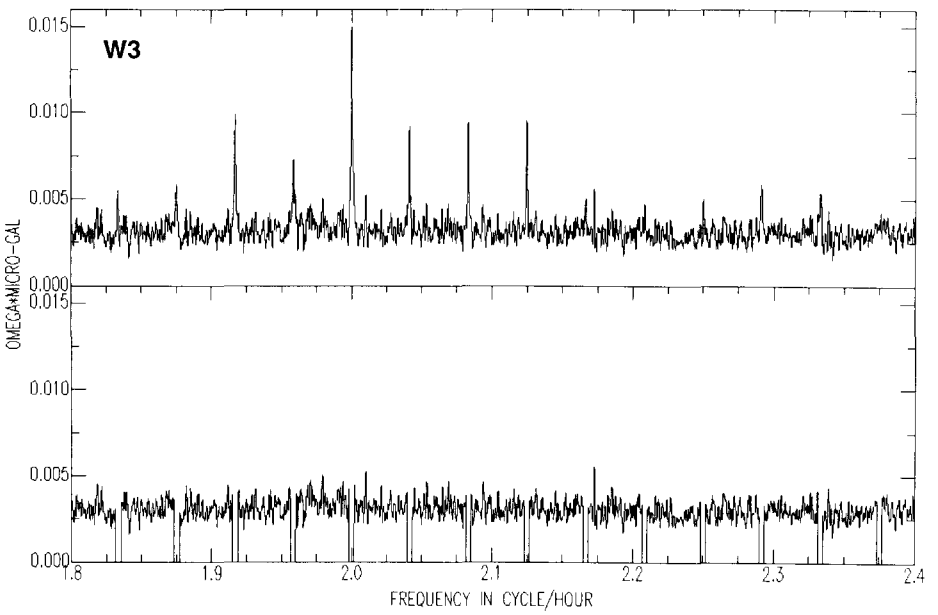

Fig. 8. Magnification of window W3 from Fig. 5. In the lower part, daily harmonics have been removed.

$\times 10^{-3}$ μgal = 2.5 nanogal. However, according to Crossley (1988), Slichter modes excited by earthquakes should have amplitudes even smaller than 2 nanogal. Since the frequencies of the Slichter modes are known to be highly sensitive to the density contrast at the inner-core boundary, a shift of the theoretical triplet towards higher frequencies is not excluded.

The second window W2, ranging from 0.75 to 1.2 cycles h^{-1}, is plotted on Fig. 7 and again shows the presence of daily harmonics. There are no other significant spectral lines. From a statistical point of view, the spectrum behaves like random noise. If we select one frequency in the spectrum, we know that the probability of the occurrence of a spectral line with an amplitude larger than twice the r.m.s. value is about 5%. Hence about 5% of the spectral lines should be larger than twice the r.m.s. value. Taking the spectrum, it is clear that one can expect many peaks to exceed such an amplitude. The same kind of remark applies to the window W3 (1.8–2.4 cycles h^{-1}) plotted in Fig. 8, where the most prominent remaining peak is at 27.6 min. This shows the difficulty of identifying new modes with certainty even in a low-noise residual gravity spectrum (see also Melchior and Ducarme, 1986; Richter, 1986; Melchior et al., 1988; Zürn et al., 1987; Mansinha et al., 1990).

Conclusion

In this preliminary analysis of the results of 1.5 years of data from the Strasbourg superconducting gravimeter, different spectral domains have been investigated. For periods between 7 h and one day, a residual gravity spectrum has been obtained by de-spiking the raw gravity record (hourly values) before and after a standard least-squares tidal analysis. By proceeding iteratively, we could reduce the residual noise in the non-tidal band to about 3 nanogal. The higher residual noise in the tidal band, reaching 20 nanogal, reflects our inability to accurately model the tidal amplitudes and phases in the presence of other contaminating signals. There is no clear evidence for any non-tidal peak in this frequency range. The local pressure signal is shown to contain harmonics of the solar day S_1 up to S_{13}. By taking the time derivative of this signal and stacking daily intervals throughout the registration period, the presence of these harmonics appears more clearly. Additionally, there seems to be a change (around 3 cycles day^{-1}) in the frequency dependence of the barometric noise which needs to be confirmed. In the analysis of periods shorter than 7 hours, we first take the time derivative of the pressure-corrected gravity signal (sampled every 5 min) in order to compensate the general shape of the noise. The signal is then high-passed to remove the tidal constituent. Most of the spectral lines present in the residual gravity spectrum are shown to be harmonics of the solar day. After removal of these harmonics, there are a few peaks in the gravity spectrum (especially a triplet around 4 h possibly related to the translational motion of the inner core) which are only marginally significant from a statistical point of view. The clear identification of similar spectral features using the records of different superconducting gravimeters (stacking method) would be of fundamental importance and could help to separate decisively local effects from global gravity changes of geophysical interest.

Ackowledgements

We warmly thank W. Zürn who helped us in the tidal analysis with the HYCON program and provided useful suggestions for improving the manuscript. Interesting and fruitful discussions with P. Rydelek, W. Zürn, H.G. Wenzel, B. Richter, G. Jentsch are acknowledged. This study was supported by INSU-CNRS, France and is DBT (Couplage global) contribution number 244.

Appendix: estimate of the spectral noise due to spikes.

To illustrate the loss of accuracy caused by a time impulse (δ function) added to a pure

harmonic function, let us first calculate the Discrete Fourier Transform (DFT) of such a signal.

The DFT of a discrete signal x_m ($m = 0, 1, \ldots N-1$) is defined for $n = 0$ to $(N-1)$ by:

$$X_n = \frac{1}{N} \sum_{m=0}^{N-1} x_m \, e^{-2\pi i n m/N}$$

Let x be a pure harmonic function of amplitude B plus an impulse of amplitude A located at $m = k$:

$$x_m = A\delta_{k-m} + B \, e^{2\pi i m p/N}$$

where $\omega = 2\pi p/N$ and where δ_{k-m} is the discrete Dirac function (0 if $k \neq m$).

Performing the DFT of x yields:

$$X_n = \frac{A}{N} e^{-2\pi i k n/N} \quad \text{if } p \neq n$$

$$X_p = \frac{A}{N} e^{-2\pi i k p/N} + B \quad \text{if } p = n$$

Hence, the spectral line squared amplitude at our frequency is:

$$|X_p|^2 = \frac{A^2}{N^2} + 2\frac{AB}{N}\cos(2\pi k p/N) + B^2$$

and the estimated amplitude of the wave can be written:

$$|X_p| = B\sqrt{\left[1 + 2R\cos(2\pi k p/N) + R^2\right]}$$

$$\text{with } R = \frac{A}{BN}$$

Assuming that $R \ll 1$,

$$|X_p| \approx B\left(1 + R\cos\phi + \frac{R^2 \sin^2\phi}{2}\right)$$

The quantity $\phi = 2\pi k p/N$ is a random variable taking any value between 0 and 2π, depending on the value of k, itself assumed to be random. Hence, the expectation of $|X_p|$ is:

$$E\left[|X_p|\right] = B\left(1 + \frac{R^2}{4}\right)$$

since the expectation of $\cos\phi$ equals 0 and that of $\sin^2\phi$ equals 1/2.

The variance of the amplitude is then given by:

$$E\left[\left(|X_p| - E[|X_P|]\right)^2\right]$$

$$= E\left[\left\{B\left(1 + R\cos\phi + \frac{R^2\sin^2\phi}{2}\right) - B\left(1 + \frac{R^2}{4}\right)\right\}^2\right]$$

To the main order of approximation, we have:

$$R^2B^2E\left[\cos^2\phi\right] = \frac{R^2B^2}{2} = \frac{A^2}{2N^2}$$

The r.m.s. error in the amplitude is simply:

$$\text{expected error} = \frac{A}{\sqrt{2}\,N}$$

We now consider a practical example. N should be considered as the number of degrees of freedom in the spectrum. Taking a sampling interval equal to unity, N equals the duration T of the signal, that is to say the number of samples. Since the signal is generally tapered by a Hann window, it is preferable to take $N = T/2$. Assume that we have $x\%$ of the signal disturbed by transient signals (5% is realistic) of equal amplitude A. The spectra of individual delta-like functions are random noise which has to be added (we exclude any periodicity in the occurence of the spikes). The standard deviation is then proportional to the square root of x. Finally, the error expected in the amplitude of any spectral line is:

$$\text{expected error} = \frac{A}{\sqrt{2}\,N}\sqrt{xN} = A\sqrt{\frac{x}{2N}}$$

For instance, $N = 24 \times 365 = 8760$ hourly data points, $A = 10$ μgal, $x = 0.05$ leads to an absolute error of 17 nanogal. This is compatible with the reduction of the noise observed in the spectra of de-spiked signals described in the text.

References

Beroza, G.C. and Jordan, T.H., 1990. Searching for slow and silent earthquakes using free oscillations. J. Geophys. Res., 95 (B3): 2845–2510.

Chapman, S. and Lindzen, R.S., 1970. Atmospheric Tides. Reidel, Dordrecht, 200 pp.

Crossley, D.J., 1988, The excitation of core modes by earthquakes. In: D.E. Smylie and R. Hide (Editors), Structure and Dynamics of Earth's Deep Interior. Geophys. Monogr. Am. Geophys. Union, 46 (1): 41–50.

Dahlen, F.A. and Sailor, R.V., 1979. Rotational and elliptical splitting of the free oscillations of the Earth. Geophys. J. R. Astron. Soc., 58: 609–623.

Haurwitz, B. and Cowley, A.D., 1973. The diurnal and semidiurnal barometric oscillations, global distribution and annual variation. Pageoph, 102: 193–222.

Hinderer, J. and Legros, H., 1989. Elasto-gravitational deformation, relative gravity changes and earth dynamics. Geophys. J., 97: 481–495.

Kikuchi, N., 1971. Annual and yearly variations of the atmospheric pressure and the Earth's rotation. Proc. Int. Lat. Obs. Mizusawa, 11: 11–28.

Legros, H. and Hinderer, J., 1990. On some perturbations of diurnal tidal waves and related nutations. Proc. 11th Int. Symp. on Earth Tides, 31 July–5 August 1989, Helsinki, in press.

Mansinha, L., Smylie, D.E. and Sutherland, B., 1990. Earthquakes and the spectrum of the Brussels Superconducting Gravimeter data for 1982–1986. Phys. Earth Planet. Inter., 61: 141–148.

Melchior, P.,1983. The Tides of the Planet Earth. Pergamon Press, Oxford, 641 p.

Melchior, P., Crossley, D.J., Dehant, V.P. and Ducarme, B., 1988, Have inertial waves been identified from the Earth's core? In: D.E. Smylie and R. Hide (Editors), Structure and Dynamics of Earth's Deep Interior, Geophys. Monogr. Am. Geophys. Union, 46 (1): 1–12.

Melchior, P. and Ducarme, B., 1986. Detection of inertial gravity oscillations in the Earth's core with a superconducting gravimeter at Brussels. Phys. Earth Planet. Inter., 36: 1–16.

Richter, B., 1983. The long-period tides in the Earth tide spectrum, XVIII IUGG General Assembly, 15–27 August 1983, Hamburg, Proc. IAG Symposia, 1: 204–216.

Richter, B., 1986. The spectrum of a registration with a superconducting gravimeter. In: R. Vieira (Editor), Proc. 10th Int. Symp. Earth Tides, 23–25 September 1985, Madrid, Consejo Superior de Investigaciones Cientificas, Madrid, pp. 131–139.

Spratt, R.S., 1982. Modelling the effect of atmospheric pressure variations on gravity. Geophys. J. R. Astron. Soc., 71: 173–186.

Schüller, K., 1977, Standard tidal analysis and its modification by frequency domain convolution. In: M. Bonatz and P. Melchior (Editors), Proc. 8th Int. Symp. on Earth Tides, 19–24 September 1977, Bonn, Institut für Theoretische Geodäsie der Universität Bonn, Bonn, pp. 94–102.

Schüller, K., 1986, Simultaneous tidal and multi-channel input analysis as implemented in the HYCON method. In: R. Vieira (Editor), Proc. 10th Int. Symp. Earth Tides, Madrid, pp. 515–520.

Volland, H., 1988. Atmospheric Tidal and Planetary Waves, Kluwer, Dordrecht, 348 pp.

Van Dam, T.M. and Wahr, J.M., 1987. Displacements of the Earth's surface due to atmospheric loading: effects on gravity and baseline measurements. J. Geophys. Res., 92: 1281–1286.

Warburton, R.J. and Goodkind, J.M., 1977. The influence of barometric pressure variations on gravity. Geophys. J. R. Astron. Soc., 48: 281–292.

Wenzel, H.G. and Zürn, W., 1990. Errors of the Cartwright–Tayler–Edden 1973 tidal potential displayed by gravimetric Earth tide observations at BFO Schiltach. Bull. Inf. Marées Terrestres, 107: 7559–7574.

Zürn, W., Richter, B., Rydelek, P.A. and Neuberg, J., 1987. Detection of inertial gravity oscillations in the Earth's core with a superconducting gravimeter at Brussels–Comment. Phys. Earth Planet. Inter., 49: 176–178.